Int J Theor Phys (2007) 46: 3135–3149
DOI 10.1007/s10773-007-9428-9

The Wigner Function and the Husimi Function of the One- and Two-Mode Combination Squeezed State

Qin Guo

Published online: 6 June 2007

Abstract In this paper we study the character of the Wigner function and Husimi function of the one- and two mode combining squeezed state (*OTCSS*) on the basis of plotting the three dimensional graphics of the Wigner function and Husimi function. It is easy to calculate the Husimi function of the OTCSS in entangled two-mode state by virtue of the formula of entangled two-mode Husimi operator: $\Delta_h(\sigma,\gamma;\kappa) = |\sigma,\gamma\rangle_{\kappa\kappa}\langle\sigma,\gamma|$ (Fan, H.-Y., Guo, Q. in Phys. Lett. A 358:203–210, 2006). It is clearly found that the evolution law of Husimi function of *OTCSS* is different from the Wigner function.

Keywords One- and two mode combining squeezed state (*OTCSS*) · Wigner function · Husimi function

1 Introduction

The squeezed states [1–6] of light play the important role in quantum optics and in potential applications to gravitational-wave detectors. Formally, these states are generated from the coherent state by appropriate squeezing operators. Such as the one-mode squeezing transformation

$$a \to a\cosh\lambda - a^{\dagger}e^{i\theta}\sinh\lambda \tag{1}$$

and two-mode squeezing transformation

$$a \to a\cosh\lambda - e^{i\theta}b^{\dagger}\sinh\lambda, \qquad b \to b\cosh\lambda - e^{i\theta}a^{\dagger}\sinh\lambda, \tag{2}$$

Work supported by the specialized research fund for the doctoral progress of higher education in China.

Q. Guo (✉)
Department of Physics, Shanghai Jiao Tong University, Shanghai 200030, China
e-mail: guoqin@sjtu.edu.cn

Q. Guo
Department of Physics, Jiangxi Normal University, Nanchang, Jiangxi 330022, China

where $a^{\dagger}(a)$ and $b^{\dagger}(b)$ are creation (annihilation) operators of two-mode harmonic oscillators. In Ref. [7] the one- and two-mode combination squeezing transformation

$$\begin{aligned} a &\to a' = a\cosh\lambda + \sinh\lambda(b\sinh r - b^{\dagger}\cosh r), \\ b &\to b' = b\cosh\lambda + \sinh\lambda(-a\sinh r - a^{\dagger}\cosh r), \end{aligned} \tag{3}$$

is discussed by virtue of the technique of integration within an ordered product (*IWOP*) [8–13]. It is a significative thing to study the characters of the one- and two-mode combination squeezed state (*OTCSS*), which is a more general type of squeezed state. Wigner function [14] and Husimi function [15] in phase space have been the important statistical methods for studying fields in quantum optics. In this paper we shall derive Wigner function and Husimi function of the *OTCSS*. Theoretical calculation and analysis on this topic will put forward a reference and comparison to the experimental measurement. In Sect. 2 we briefly introduce the character of the one- and two-mode combination squeezing transformation operator U, in Sect. 3 we calculate the Wigner function of *OTCSS*, in Sect. 4 we obtain the marginal distribution of Wigner operator in the *OTCSS* and then we plot the three dimensional graphics of the Wigner function W_{OT} in Sect. 5. In Sect. 6 we calculate the Husimi function of *OTCSS*, and plot the three dimensional graphics of the Husimi function H_{OT} in Sect. 7. In so doing the physical significance of the Wigner function and the Husimi function of the *OTCSS* is revealed completely.

2 The One- and Two-Mode Combination Squeezing Transformation Operator U

The one- and two-mode combination squeezing transformation (3) is equivalent to the following unitary transformation U,

$$\begin{aligned} Q_1 &\to Q_1' = UQ_1U^{-1} = Q_1\cosh\lambda - Q_2e^{-r}\sinh\lambda, \\ Q_2 &\to Q_2' = UQ_2U^{-1} = Q_2\cosh\lambda - Q_1e^{r}\sinh\lambda, \\ P_1 &\to P_1' = UP_1U^{-1} = P_1\cosh\lambda + P_2e^{r}\sinh\lambda, \\ P_2 &\to P_2' = UP_2U^{-1} = P_2\cosh\lambda + P_1e^{-r}\sinh\lambda, \end{aligned} \tag{4}$$

where U is called one- and two-mode combination squeezing transformation operator. Accordingly, under the same transformation the base vector must so behave

$$U|q_1, q_2\rangle = |q_1\cosh\lambda + q_2e^{-r}\sinh\lambda, q_2\cosh\lambda + q_1e^{r}\sinh\lambda\rangle \equiv |q_1, q_2\rangle' \tag{5}$$

as to keep the eigenvalues invariant; e.g.,

$$\begin{aligned} (Q_1\cosh\lambda - Q_2e^{-r}\sinh\lambda)|q_1, q_2\rangle' &= q_1|q_1, q_2\rangle', \\ (Q_2\cosh\lambda - Q_1e^{r}\sinh\lambda)|q_1, q_2\rangle' &= q_2|q_1, q_2\rangle'. \end{aligned} \tag{6}$$

Combing (5) and $\iint_{-\infty}^{\infty} dq_1dq_2|q_1, q_2\rangle\langle q_1, q_2| = 1$, we identify U with the following coordinate representation,

$$\begin{aligned} U &= \iint_{-\infty}^{\infty} dq_1dq_2|q_1\cosh\lambda + q_2e^{-r}\sinh\lambda, q_2\cosh\lambda + q_1e^{r}\sinh\lambda\rangle\langle q_1, q_2| \\ &= \iint_{-\infty}^{\infty} dq_1dq_2\left|R\begin{bmatrix} q_1 \\ q_2 \end{bmatrix}\right\rangle\left\langle\begin{bmatrix} q_1 \\ q_2 \end{bmatrix}\right| \equiv U(R), \end{aligned} \tag{7}$$

$$R=\begin{bmatrix}\cosh\lambda & e^{-r}\sinh\lambda\\ e^{r}\sinh\lambda & \cosh\lambda\end{bmatrix},\qquad \left|\begin{bmatrix}q_1\\ q_2\end{bmatrix}\right\rangle\equiv|q_1,q_2\rangle,\qquad \det R=1,$$

where λ and r are real, U is unitary

$$U^{\dagger}U=\iint_{-\infty}^{\infty}dq_1dq_2\left|R\begin{bmatrix}q_1\\ q_2\end{bmatrix}\right\rangle\left\langle R\begin{bmatrix}q_1\\ q_2\end{bmatrix}\right|=1=UU^{\dagger}.$$

3 The Wigner Function of the One- and Two-Mode Combination Squeezed State

Applying the one- and two-mode combination squeezing operator U

$$U=\iint_{-\infty}^{\infty}dq_1dq_2|q_1\cosh\lambda+e^{-r}q_2\sinh\lambda,q_2\cosh\lambda+e^{r}q_1\sinh\lambda\rangle\langle q_1,q_2| \tag{8}$$

on the two-mode vacuum state $|00\rangle$, we obtain $U|00\rangle$, which is called the one- and two-mode combination squeezed state (*OTCSS*). According to the definition of Wigner operator:

$$\Delta(p,q)=\int_{-\infty}^{\infty}\frac{du}{2\pi}e^{ipu}\left|q+\frac{u}{2}\right\rangle\left\langle q-\frac{u}{2}\right|, \tag{9}$$

we have

$$\begin{aligned}&\Delta(p_1,q_1)\Delta(p_2,q_2)\\ &\quad=\int_{-\infty}^{\infty}\frac{du}{2\pi}e^{ip_1u}\int_{-\infty}^{\infty}\frac{du'}{2\pi}e^{ip_2u'}\left|q_1+\frac{u}{2},q_2+\frac{u'}{2}\right\rangle\left\langle q_1-\frac{u}{2},q_2-\frac{u'}{2}\right|.\end{aligned} \tag{10}$$

Then the Wigner function of the *OTCSS* can be gotten through the following calculation,

$$\begin{aligned}W_{OT}&=\langle\psi|\Delta(p_1,q_1)\Delta(p_2,q_2)|\psi\rangle\\ &=\langle00|U^{-1}\Delta(p_1,q_1)\Delta(p_2,q_2)U|00\rangle\\ &=\iint_{-\infty}^{\infty}dq_1''dq_2''\langle00||q_1'',q_2''\rangle\langle q_1''\cosh\lambda+e^{-r}q_2''\sinh\lambda,q_2''\cosh\lambda+e^{r}q_1''\sinh\lambda|\\ &\quad\times\int_{-\infty}^{\infty}\frac{du}{2\pi}e^{ip_1u}\left|q_1+\frac{u}{2}\right\rangle\left\langle q_1-\frac{u}{2}\right|\int_{-\infty}^{\infty}\frac{du'}{2\pi}e^{ip_2u'}\left|q_2+\frac{u'}{2}\right\rangle\left\langle q_2-\frac{u'}{2}\right|\\ &\quad\times\iint_{-\infty}^{\infty}dq_1'dq_2'|q_1'\cosh\lambda+e^{-r}q_2'\sinh\lambda,q_2'\cosh\lambda+e^{r}q_1'\sinh\lambda\rangle\langle q_1',q_2'||00\rangle\\ &=\frac{1}{4\pi^2}\iint_{-\infty}^{\infty}e^{ip_1u}e^{ip_2u'}dudu'\iint_{-\infty}^{\infty}dq_1''dq_2''\iint_{-\infty}^{\infty}dq_1'dq_2'\langle00||q_1'',q_2''\rangle\langle q_1',q_2'||00\rangle\\ &\quad\times\langle q_1''\cosh\lambda+e^{-r}q_2''\sinh\lambda,q_2''\cosh\lambda+e^{r}q_1''\sinh\lambda|\left|q_1+\frac{u}{2},q_2+\frac{u'}{2}\right\rangle\\ &\quad\times\left\langle q_1-\frac{u}{2},q_2-\frac{u'}{2}\right|q_1'\cosh\lambda+e^{-r}q_2'\sinh\lambda,q_2'\cosh\lambda+e^{r}q_1'\sinh\lambda\rangle,\end{aligned} \tag{11}$$

where $|\psi\rangle$ is $U|00\rangle$. Substituting the orthonormal relation between the coordinate eigenstates $|q\rangle$

$$\langle q'|q\rangle = \delta(q'-q) \tag{12}$$

into (11), we have

$$\begin{aligned}
&\langle\psi|\Delta(p_1,q_1)\Delta(p_2,q_2)|\psi\rangle \\
&= \frac{1}{4\pi^2}\iint_{-\infty}^{\infty} e^{ip_1u}e^{ip_2u'}dudu' \iint_{-\infty}^{\infty} dq_1''dq_2'' \\
&\quad\times \iint_{-\infty}^{\infty} dq_1'dq_2'\frac{1}{\pi}\exp\left(-\frac{q_1''^2+q_2''^2}{2}\right)\exp\left(-\frac{q_1'^2+q_2'^2}{2}\right) \\
&\quad\times \delta\left(q_1''\cosh\lambda + e^{-r}q_2''\sinh\lambda - q_1 - \frac{u}{2}\right)\delta\left(q_2''\cosh\lambda + e^{r}q_1''\sinh\lambda - q_2 - \frac{u'}{2}\right) \\
&\quad\times \delta\left(q_1 - \frac{u}{2} - q_1'\cosh\lambda - e^{-r}q_2'\sinh\lambda\right)\delta\left(q_2 - \frac{u'}{2} - q_2'\cosh\lambda - e^{r}q_1'\sinh\lambda\right).
\end{aligned} \tag{13}$$

After integrating over q_1'', q_2'', q_1', q_2' respectively, we obtain the following compact result.

$$\begin{aligned}
&\langle 00|U^{-1}\Delta(p_1,q_1)\Delta(p_2,q_2)U|00\rangle \\
&= \frac{1}{4\pi^3}\iint_{-\infty}^{\infty} dudu'\exp\Big[-q_1^2L_1 - \frac{u^2}{4}L_1 - q_2^2L_2 - \frac{u'^2}{4}L_2 + uu'L_3 \\
&\quad + 4q_1q_2L_3 + ip_1u + ip_2u'\Big],
\end{aligned} \tag{14}$$

where L_1, L_2 and L_3 are:

$$\begin{aligned}
L_1 &\equiv \cosh^2\lambda + \sinh^2\lambda e^{2r}, \\
L_2 &\equiv \cosh^2\lambda + \sinh^2\lambda e^{-2r}, \\
L_3 &\equiv \cosh\lambda\sinh\lambda\cosh r.
\end{aligned} \tag{15}$$

Then integrating (14) over u and u', we obtain the Wigner function of the *OTCSS*

$$\begin{aligned}
W_{OT} &= \langle 00|U^{-1}\Delta(p_1,q_1)\Delta(p_2,q_2)U|00\rangle \\
&= \frac{1}{\pi^2\sqrt{L_1L_2-4L_3^2}} \\
&\quad\times\exp\Big[-\frac{1}{L_1L_2-4L_3^2}(L_1p_2^2 + L_2p_1^2 + 4p_1p_2L_3) - (q_1^2L_1 + q_2^2L_2 - 4q_1q_2L_3)\Big].
\end{aligned} \tag{16}$$

4 The Marginal Distribution of Wigner Operator in the One- and Two-Mode Combination Squeezed State

Among various phase space distributions the Wigner function is the most popularly used, since its two marginal distributions lead to measuring probability density in coordinate space and momentum space respectively. So we calculate the marginal distribution of Wigner operator in the *OTCSS*. The marginal distribution of Wigner function in the coordinate "q-direction" is

$$\begin{aligned} W_q &= \iint_{-\infty}^{\infty} dp_1 dp_2 W_{OT} = \langle 00|U^{-1} \iint_{-\infty}^{\infty} dp_1 dp_2 \Delta(p_1, q_1)\Delta(p_2, q_2) U|00\rangle \\ &= \frac{1}{\pi^2} \frac{1}{\sqrt{L_1 L_2 - 4L_3^2}} \iint_{-\infty}^{\infty} dp_1 dp_2 \\ &\quad \times \exp\left[-\frac{1}{L_1 L_2 - 4L_3^2} (L_1 p_2^2 + L_2 p_1^2 + 4 p_1 p_2 L_3) - (q_1^2 L_1 + q_2^2 L_2 - 4 q_1 q_2 L_3) \right] \\ &= \frac{1}{\pi} \exp[-(q_1^2 L_1 + q_2^2 L_2 - 4 q_1 q_2 L_3)]. \end{aligned} \tag{17}$$

The marginal distribution of Wigner function in the coordinate "p-direction" is

$$\begin{aligned} W_p &= \iint_{-\infty}^{\infty} dq_1 dq_2 W_{OT} = \langle 00|U^{-1} \iint_{-\infty}^{\infty} dq_1 dq_2 \Delta(p_1, q_1)\Delta(p_2, q_2) U|00\rangle \\ &= \frac{1}{\pi^2} \frac{1}{\sqrt{L_1 L_2 - 4L_3^2}} \iint_{-\infty}^{\infty} dq_1 dq_2 \\ &\quad \times \exp\left[-\frac{1}{L_1 L_2 - 4L_3^2} (L_1 p_2^2 + L_2 p_1^2 + 4 p_1 p_2 L_3) - (q_1^2 L_1 + q_2^2 L_2 - 4 q_1 q_2 L_3) \right] \\ &= \frac{1}{\pi} \frac{1}{L_1 L_2 - 4L_3^2} \exp\left[-\frac{1}{L_1 L_2 - 4L_3^2} (L_1 p_2^2 + L_2 p_1^2 + 4 p_1 p_2 L_3) \right]. \end{aligned} \tag{18}$$

5 The Three-Dimensional Graphics of the Wigner Function W_{OT}

In order to study the Wigner function distribution of the one- and two-mode combination squeezed state, We have plot the three-dimensional graphics of the Wigner function W_{OT}. For there are four variables q_1, p_1, q_2, p_2 in the formula of the Wigner function W_{OT}, we let q_2, p_2 take some definite value at first and study the distribution law of the Wigner function W_{OT} varying with the variables q_1, p_1. Then we let q_1, p_1 take some definite value and study the distribution law of the Wigner function W_{OT} varying with the variables q_2, p_2. In the following discussion, we also study the influence of the squeezing parameter λ and the one- and two-mode combining parameter r on the Wigner function W_{OT}.

First let's study the influence of the squeezing parameter λ on the Wigner function distribution. In Fig. 1, we have plotted the three dimensional graphics of the Wigner function varying with the variables q_1, p_1 ($W(q_1, p_1)$) for different value of λ while $r = 0$ and

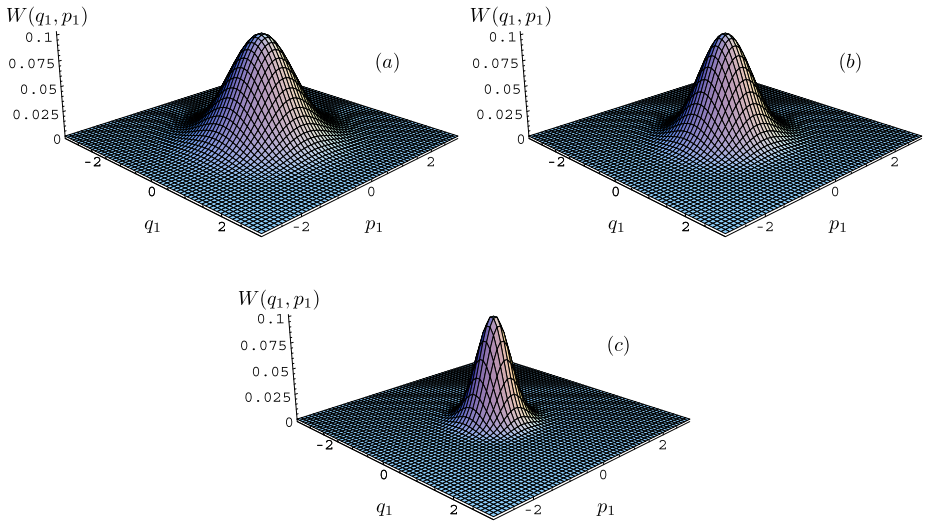

Fig. 1 The Wigner function of the OTCSS for $q_2 = 0$, $p_2 = 0$, $r = 0$ and different value of the squeezing parameter λ: (**a**) $\lambda = 0$, (**b**) $\lambda = 0.5$, (**c**) $\lambda = 1$

$q_2 = 0$, $p_2 = 0$. When $\lambda = 0$ and $r = 0$, $q_2 = 0$, $p_2 = 0$ (Fig. 1(a)), the Wigner function ($W(q_1, p_1)$) is a round hill located at ($q_1 = 0$, $p_1 = 0$), which is just the Wigner function (W_{vac}) of the vacuum state. When $\lambda = 0$, we have: $L_1 = L_2 = 1$, $L_3 = 0$, so $W_{OT}|_{\lambda=0} = \frac{1}{\pi^2} \exp[-p_1^2 - q_1^2 - p_2^2 - q_2^2] = W_{\text{vac}}$, it is a special case of the Wigner function of the *OTCSS*. In the case of $r = 0$, $\lambda \neq 0$ (see Fig. 1(b),(c)), $W(q_1, p_1)$ is the Wigner function of the two-mode squeezed state. Because when $r = 0$, the one- and two-mode combination squeezing transformation

$$a \to a' = a\cosh\lambda + \sinh\lambda(b\sinh r - b^\dagger \cosh r) \overset{r=0}{=} a\cosh\lambda - \sinh\lambda b^\dagger,$$

$$b \to b' = b\cosh\lambda + \sinh\lambda(-a\sinh r - a^\dagger \cosh r) \overset{r=0}{=} b\cosh\lambda - \sinh\lambda a^\dagger$$

become the two-mode squeezing transformation. Comparing with Fig. 1(c) and Fig. 1(b), we find that with the increasing of the squeezing parameter λ, the Wigner function is becoming steeper. It shows that the squeezing parameter influence the distribution scope of the Wigner function; the bigger the value of the squeezing parameter, the more narrow the distribution scope is.

In Fig. 2, we have plotted the three dimensional graphics of the Wigner function $W(q_1, p_1)$ varying with the variables q_1, p_1 for different value of parameter λ while $r = 1$ and $q_2 = 0$, $p_2 = 0$. In the case of $r \neq 0$ and $\lambda \neq 0$, $W(q_1, p_1)$ is the Wigner function of the *OTCSS*. Comparing with Fig. 2(a) ($r = 1$, $\lambda = 0.5$) and Fig. 1(b) ($r = 0, \lambda = 0.5$), we clearly see that the plot along q-axis direction is squeezed under the action of the one- and two-mode combining parameter r (see Fig. 2(a)). Comparing with the three plots in Fig. 2, we find that as the value of squeezing parameter λ increasing, the squeezing degree of whole plot get deeper. Not only the distribution scope of the Wigner function become more narrow but also the peak value become lower.

Next let's discuss the influence of the one- and two-mode combining parameter r on the Wigner function distribution. In Fig. 3, we have plotted the three dimensional graphics of the

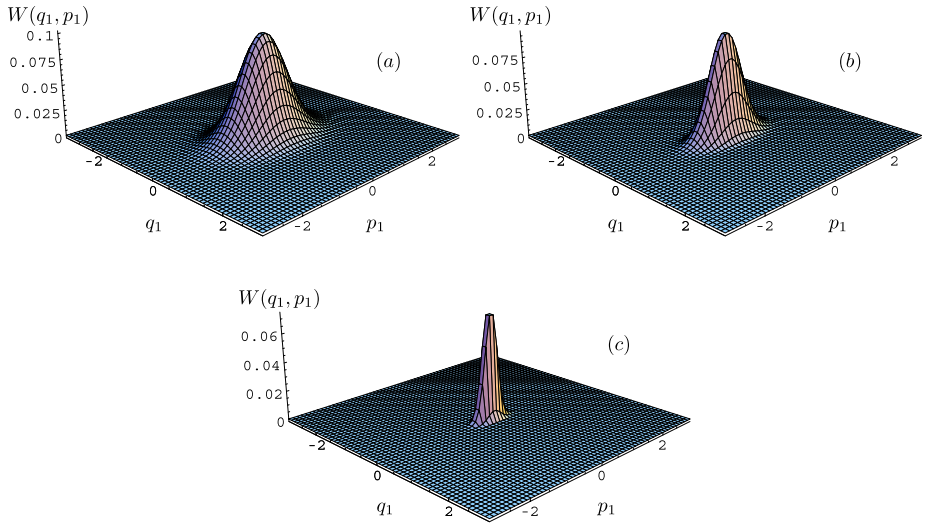

Fig. 2 The Wigner function of the OTCSS for $q_2 = 0$, $p_2 = 0$, $r = 1$ and different value of the squeezing parameters λ: (**a**) $\lambda = 0.5$, (**b**) $\lambda = 1$, (**c**) $\lambda = 2$

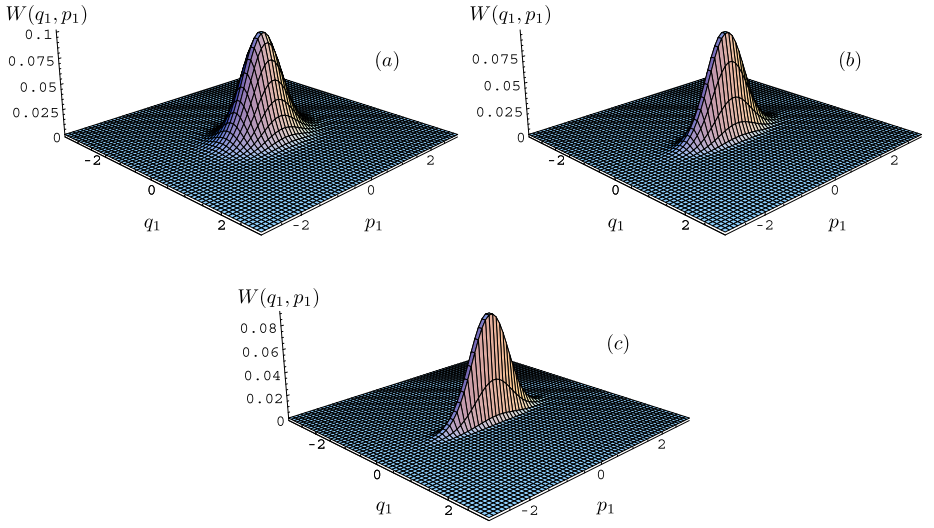

Fig. 3 The Wigner function of the OTCSS for $q_2 = 0$, $p_2 = 0$, $\lambda = 0.8$ and different value of r: (**a**) $r = 0.6$, (**b**) $r = 1.4$, (**c**) $r = 2.0$

Wigner function $W(q_1, p_1)$ varying with the variables q_1, p_1 for different value of parameter r while $\lambda = 0.8$ and $q_2 = 0$, $p_2 = 0$. Comparing with the three plots in Fig. 3, we find that with the increasing of the value of parameter r, the squeezing degree of the plot along q-axis direction get deeper, while the plot along p-axis direction is not squeezed.

In Fig. 4 and Fig. 5, we study the influence of different value of q_2 and p_2 on the Wigner function $W(q_1, p_1)$. In Fig. 4, we can see that when we maintain the value of r, λ, p_2, and

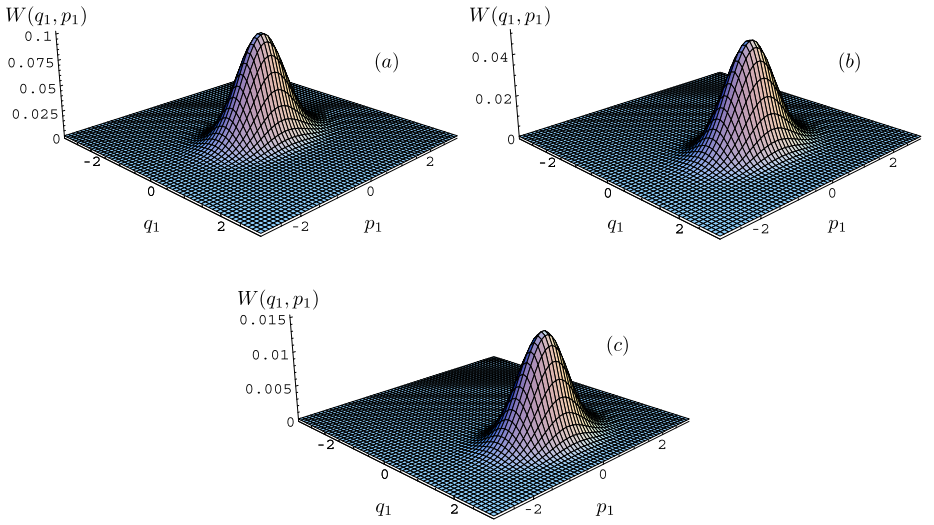

Fig. 4 The Wigner function of the OTCSS for $p_2 = 0$, $r = 1$, $\lambda = 0.5$ and different value of q_2: (**a**) $q_2 = 0$, (**b**) $q_2 = 1.5$, (**c**) $q_2 = 2.5$

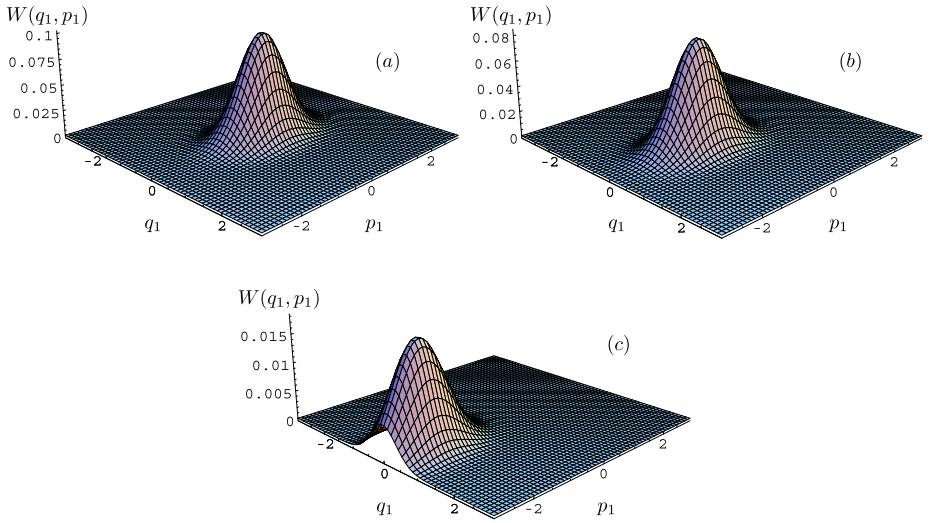

Fig. 5 The Wigner function of the OTCSS for $q_2 = 0$, $r = 1$, $\lambda = 0.5$ and different value of p_2: (**a**) $p_2 = 0$, (**b**) $p_2 = 0.5$, (**c**) $p_2 = 1.5$

take $q_2 = 0, 1.5, 2.5$ respectively, the wave crest move apart from the center and toward the positive direction of coordinate q_1 and the height of the hill are declining simultaneously. In Fig. 5, we can see that when we maintain the value of r, λ, q_2, and take $p_2 = 0, 0.5, 1.5$ respectively, the wave crest moves apart from the center and toward the negative direction of p_1 and the height of the hill is declining simultaneously.

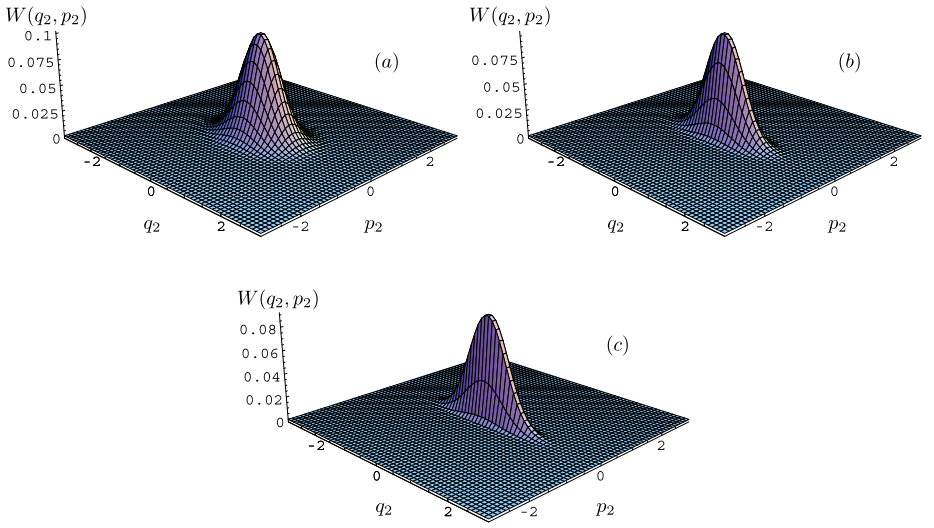

Fig. 6 The Wigner function of the OTCSS for $q_1 = 0$, $p_1 = 0$, $\lambda = 0.8$ and different value of r: (**a**) $r = 0.6$, (**b**) $r = 1.4$, (**c**) $r = 2.0$

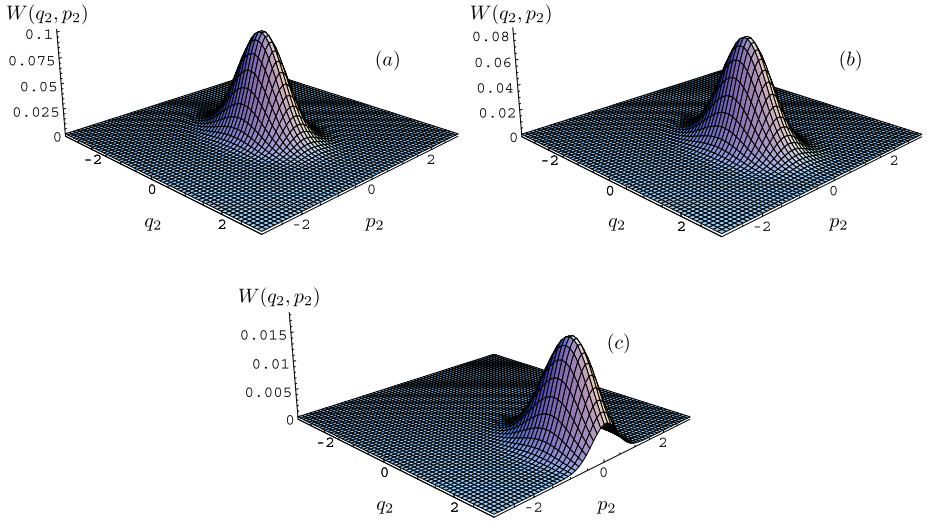

Fig. 7 The Wigner function of the OTCSS for $p_1 = 0$, $r = 1$, $\lambda = 0.5$ and different value of q_1: (**a**) $q_1 = 0$, (**b**) $q_1 = 0.5$, (**c**) $q_1 = 1.5$

We also plot the three dimensional graphics of the Wigner function varying with the variables q_2, p_2 ($W(q_2, p_2)$), which can be seen in Fig. 6 and Fig. 7. The influence of squeezing parameter λ on the Wigner function $W(q_2, p_2)$ is similar with $W(q_1, p_1)$. The difference between $W(q_2, p_2)$ and $W(q_1, p_1)$ lie in the squeezing direction of the plot. We clearly see that the plot ($W(q_2, p_2)$) along p-axis direction is squeezed when $r \neq 0$ and $\lambda \neq 0$ (see Fig. 6

and Fig. 7), while the plot $(W(q_1, p_1))$ along q-axis direction is squeezed when $r \neq 0$ and $\lambda \neq 0$ (see Figs. 2, 3, 4, 5).

In Fig. 6, we have plotted the three dimensional graphics of $W(q_2, p_2)$ varying with the variables q_2, p_2 for different value of r while $\lambda = 0.8$ and $q_1 = 0$, $p_1 = 0$. Comparing with the three plots in Fig. 6, we find that as the value of r is increasing, the squeezing degree of the plot along p-axis direction get deeper, while the plot along q-axis direction is not squeezed; which is different with the evolution rule of $W(q_1, p_1)$ (see Fig. 3).

In Fig. 7, we have plotted the three dimensional graphics of $W(q_2, p_2)$ varying with the variables q_2, p_2 for different value of q_1 while $r = 1$, $\lambda = 0.5$, and $p_1 = 0$. We can see that when we maintain the value of r, λ, p_1, and take $q_1 = 0, 0.5, 1.5$ respectively, the hill move apart from the center and toward the positive direction of coordinate q_2 and the height of the hill is declining simultaneously. Comparing with Fig. 7 and Fig. 5, it is interesting to find that the evolution rule of $W(q_2, p_2)$ under the different value of coordinate q_1 (see Fig. 7) is similar with one of $W(q_1, p_1)$ under the different value of momentum p_2 (see Fig. 5). We can also find this same interesting phenomena in the evolution rule of $W(q_2, p_2)$ under the different value of momentum p_1 (which is not listed in this paper) and $W(q_1, p_1)$ under the different value of coordinate q_2 (see Fig. 4).

6 The Husimi Function of the One- and Two-Mode Combination Squeezed State

In one-mode case, the Husimi distribution function $F_h(q, p, \kappa)$ is defined in a manner that it is smoothing out the Wigner function $F_w(q, p)$ by averaging over a "coarse graining" function $\exp[-\kappa|q' - q|^2 - \frac{|p'-p|^2}{\kappa}]$ [16], where κ is the Gaussian spatial width parameter, which is free to be chosen and which determines the relative resolution in p-space versus q-space. In two-mode case, we have defined the entangled two-mode Husimi operator $\Delta_h(\sigma, \gamma; \kappa)$ by smoothing out the entangled Wigner operator $\Delta_w(\sigma', \gamma')$ by averaging over a "coarse graining" function $\exp[-\kappa|\sigma' - \sigma|^2 - \frac{|\gamma'-\gamma|^2}{\kappa}]$ [17],

$$\begin{aligned}\Delta_h(\sigma, \gamma; \kappa) &= 4\int d^2\sigma' d^2\gamma' \Delta_w(\sigma', \gamma') \exp\left[-\kappa|\sigma' - \sigma|^2 - \frac{|\gamma' - \gamma|^2}{\kappa}\right] \\ &= |\sigma, \gamma\rangle_{\kappa\kappa}\langle\sigma, \gamma|. \end{aligned} \tag{19}$$

Now we study the Husimi function of the $OTCSS(H_{OT})$ in two-mode entangled state, it can be calculated by the following formula:

$$H_{OT} = \langle\Psi|\Delta_h(\sigma, \gamma; \kappa)|\Psi\rangle = \langle 00|U^{-1}|\Delta_h(\sigma, \gamma; \kappa)|U|00\rangle, \tag{20}$$

where $|\Psi\rangle = U|00\rangle$ is the $OTCSS$. Thus

$$\begin{aligned} H_{OT} &= \langle 00|U^{-1}|\Delta_h(\sigma, \gamma; \kappa)|U|00\rangle = \langle 00|U^{-1}||\sigma, \gamma\rangle_{\kappa\kappa}\langle\sigma, \gamma||U|00\rangle \\ &= |{}_\kappa\langle\sigma, \gamma|U|00\rangle|^2. \end{aligned} \tag{21}$$

Now let we calculate ${}_\kappa\langle\sigma, \gamma|U|00\rangle$. In reference [17] we have defined the two-mode squeezed coherent state,

$$|\sigma, \gamma\rangle_\kappa = S_2(1/\sqrt{\kappa})D_1(\varepsilon_1)D_2(\varepsilon_2)|00\rangle, \tag{22}$$

where $S_2(\sqrt{\kappa}) = e^{(a_1 a_2 - a_1^\dagger a_2^\dagger)\ln\sqrt{\kappa}}$ is the two-mode squeezing operator [18–22], $D_i(\varepsilon_i) = \exp[\varepsilon_i a_i^\dagger - \varepsilon_i^* a_i]|0\rangle_i$ is the displacement operator, where

$$\varepsilon_1 = \frac{\gamma/\sqrt{\kappa} + \sqrt{\kappa}\sigma}{2}, \qquad \varepsilon_2 = \frac{\gamma^*/\sqrt{\kappa} - \sqrt{\kappa}\sigma^*}{2}. \tag{23}$$

Substituting (22) and the expression of U (7) into $({}_\kappa\langle\sigma,\gamma|U|00\rangle)$, we obtain:

$${}_\kappa\langle\sigma,\gamma|U|00\rangle = \langle 00|D_1^\dagger(\varepsilon_1)D_2^\dagger(\varepsilon_2)S_2^\dagger(1/\sqrt{\kappa})\iint_{-\infty}^{\infty} dq_1 dq_2 |q_1', q_2'\rangle\langle q_1, q_2||00\rangle \tag{24}$$

where

$$q_1' = q_1\cosh\lambda + q_2 e^{-r}\sinh\lambda, q_2' = q_2\cosh\lambda + q_1 e^{r}\sinh\lambda. \tag{25}$$

Notice

$$\langle 00|D_1^\dagger(\varepsilon_1)D_2^\dagger(\varepsilon_2) = \langle\varepsilon_1,\varepsilon_2|, \langle q_1, q_2|00\rangle = \pi^{-\frac{1}{2}}\exp\left(-\frac{1}{2}q_1^2 - \frac{1}{2}q_2^2\right) \tag{26}$$

and

$$\begin{gathered} S_2^\dagger(1/\sqrt{\kappa}) = \iint_{-\infty}^{\infty} dq_1'' dq_2'' |q_1''\cosh\lambda + q_2''\sinh\lambda, q_1''\sinh\lambda + q_2''\cosh\lambda\rangle\langle q_1'', q_2''|, \\ \lambda = 1/\sqrt{\kappa}, \\ S_2^\dagger(1/\sqrt{\kappa})|q_1', q_2'\rangle = |q_1'\cosh\lambda + q_2'\sinh\lambda, q_1'\sinh\lambda + q_2'\cosh\lambda\rangle \end{gathered} \tag{27}$$

we have

$$\begin{aligned} {}_\kappa\langle\sigma,\gamma|U|00\rangle = &\iint_{-\infty}^{\infty} dq_1 dq_2 \pi^{-\frac{1}{2}}\exp\left(-\frac{1}{2}q_1^2 - \frac{1}{2}q_2^2\right) \\ &\times\langle\varepsilon_1,\varepsilon_2||q_1'\cosh\lambda + q_2'\sinh\lambda, q_1'\sinh\lambda + q_2'\cosh\lambda\rangle. \end{aligned} \tag{28}$$

Using the following formulas [23],

$$\begin{aligned} \langle q|z\rangle &= \pi^{-\frac{1}{4}}\exp\left\{-\frac{q^2}{2} - \frac{|z|^2}{2} + \sqrt{2}qz - \frac{z^2}{2}\right\}, \\ \langle z|q\rangle &= \pi^{-\frac{1}{4}}\exp\left\{-\frac{q^2}{2} - \frac{|z|^2}{2} + \sqrt{2}qz^* - \frac{z^{*2}}{2}\right\}, \end{aligned} \tag{29}$$

we obtain

$$\begin{aligned} &\langle\varepsilon_1,\varepsilon_2||q_1'\cosh\lambda + q_2'\sinh\lambda, q_1'\sinh\lambda + q_2'\cosh\lambda\rangle \\ &= \pi^{-\frac{1}{2}}\exp\left\{-\frac{(q_1'\cosh\lambda + q_2'\sinh\lambda)^2}{2} - \frac{|\varepsilon_1|^2}{2} + \sqrt{2}(q_1'\cosh\lambda + q_2'\sinh\lambda)\varepsilon_1^* - \frac{\varepsilon_1^{*2}}{2}\right\} \\ &\quad\times\exp\left\{-\frac{(q_1'\sinh\lambda + q_2'\cosh\lambda)^2}{2} - \frac{|\varepsilon_2|^2}{2} + \sqrt{2}(q_1'\sinh\lambda + q_2'\cosh\lambda)\varepsilon_2^* - \frac{\varepsilon_2^{*2}}{2}\right\}. \end{aligned} \tag{30}$$

Noting q_1', q_2' is related with q_1 and q_2, see (25), then

$$\begin{aligned}&\langle\varepsilon_1,\varepsilon_2||q_1'\cosh\lambda+q_2'\sinh\lambda,q_1'\sinh\lambda+q_2'\cosh\lambda\rangle\\&=\pi^{-\frac{1}{2}}\exp\left\{-\frac{1}{2}[q_1L_1+q_2L_2]^2-\frac{|\varepsilon_1|^2}{2}+\sqrt{2}[q_1L_1+q_2L_2]\varepsilon_1^*-\frac{\varepsilon_1^{*2}}{2}\right\}\\&\quad\times\exp\left\{-\frac{1}{2}[q_1L_2'+q_2L_1']^2-\frac{|\varepsilon_2|^2}{2}+\sqrt{2}[q_1L_2'+q_2L_1']\varepsilon_2^*-\frac{\varepsilon_2^{*2}}{2}\right\},\end{aligned}\tag{31}$$

where

$$\begin{aligned}L_1&=\cosh^2\lambda+e^r\sinh^2\lambda,\quad L_2=(e^{-r}+1)\sinh\lambda\cosh\lambda,\\L_1'&=\cosh^2\lambda+e^{-r}\sinh^2\lambda,\quad L_2'=(e^r+1)\sinh\lambda\cosh\lambda.\end{aligned}\tag{32}$$

Substituting (31) into (28), we have

$$\begin{aligned}{}_\kappa\langle\sigma,\gamma|U|00\rangle&=\pi^{-1}\iint_{-\infty}^{\infty}dq_1dq_2\exp\left\{-\frac{1}{2}q_1^2(1+L_1^2+L_2'^2)-\frac{1}{2}q_2^2(1+L_2^2+L_1'^2)\right.\\&\quad-q_1q_2(L_1L_2+L_2'L_1')+\sqrt{2}q_1(L_1\varepsilon_1^*+L_2'\varepsilon_2^*)+\sqrt{2}q_2(L_2\varepsilon_1^*+L_1'\varepsilon_2^*)\\&\quad\left.-\frac{|\varepsilon_1|^2+|\varepsilon_2|^2+\varepsilon_1^{*2}+\varepsilon_2^{*2}}{2}\right\}\\&=\frac{2}{\sqrt{A_1}}\exp\left[\varepsilon_1^{*2}\left(\frac{B_1^2}{CA_1}+\frac{L_1^2}{C}-\frac{1}{2}\right)+\varepsilon_2^{*2}\left(\frac{B_2^2}{CA_1}+\frac{L_2'^2}{C}-\frac{1}{2}\right)\right.\\&\quad\left.+2\varepsilon_1^*\varepsilon_2^*\left(\frac{B_1B_2}{CA_1}+\frac{L_1L_2'}{C}\right)\right]\exp\left(-\frac{|\varepsilon_1|^2+|\varepsilon_2|^2}{2}\right),\end{aligned}\tag{33}$$

where

$$\begin{aligned}&(1+L_1^2+L_2'^2)\equiv C,\qquad 1+L_2^2+L_1'^2+L_1^2+L_2'^2+(L_1L_1'-L_2L_2')^2\equiv A_1,\\&(L_2+L_2L_2'^2-L_1L_2'L_1')\equiv B_1,\qquad (L_1'+L_1'L_1^2-L_2'L_1L_2)\equiv B_2.\end{aligned}\tag{34}$$

Thus we obtain the Husimi function of *OTCSS*.

$$\begin{aligned}H_{OT}&=|{}_\kappa\langle\sigma,\gamma|U|00\rangle|^2\\&=\frac{4}{|A_1|}\left|\exp\left[\varepsilon_1^{*2}\left(\frac{B_1^2}{CA_1}+\frac{L_1^2}{C}-\frac{1}{2}\right)+\varepsilon_2^{*2}\left(\frac{B_2^2}{CA_1}+\frac{L_2'^2}{C}-\frac{1}{2}\right)\right.\right.\\&\quad\left.\left.+2\varepsilon_1^*\varepsilon_2^*\left(\frac{B_1B_2}{CA_1}+\frac{L_1L_2'}{C}\right)\right]\right|^2\exp[-(|\varepsilon_1|^2+|\varepsilon_2|^2)].\end{aligned}\tag{35}$$

7 The Three-Dimensional Graphics of the Husimi Function H_{OT}

Considering that ε_1 and ε_2 are complex number, we let

$$\begin{aligned}\gamma=\gamma_1+i\gamma_2,\qquad \sigma=\sigma_1+i\sigma_2,\\\varepsilon_1=\tfrac{\gamma/\sqrt{\kappa}+\sqrt{\kappa}\sigma}{2}=x_1+iy_1,\qquad \varepsilon_2=\frac{\gamma^*/\sqrt{\kappa}-\sqrt{\kappa}\sigma^*}{2}=x_2+iy_2,\end{aligned}\tag{36}$$

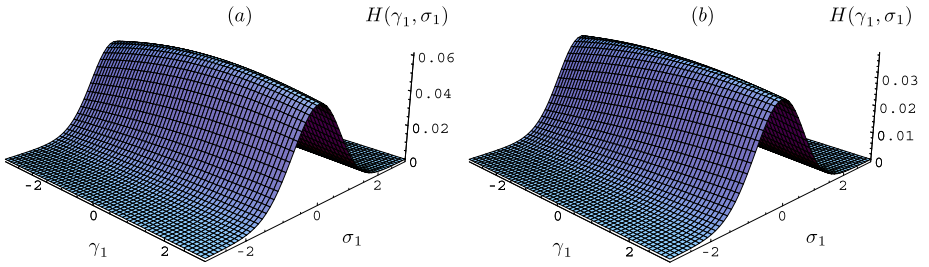

Fig. 8 The Husimi function of the OTCSS for $\gamma_2 = 0$, $\sigma_2 = 0$, $\kappa = 1$ and different value of r: (**a**) $r = \pi/6$, (**b**) $r = \pi/3$

where

$$x_1 = \frac{1}{2}\left(\gamma_1\lambda + \frac{\sigma_1}{\lambda}\right), \qquad y_1 = \frac{1}{2}\left(\gamma_2\lambda + \frac{\sigma_2}{\lambda}\right),$$
$$x_2 = \frac{1}{2}\left(\gamma_1\lambda - \frac{\sigma_1}{\lambda}\right), \qquad y_2 = -\frac{1}{2}\left(\gamma_2\lambda - \frac{\sigma_2}{\lambda}\right), \tag{37}$$

then

$$H_{OT} = \frac{4}{A_1}\exp\left[2(x_1^2 - y_1^2)\left(\frac{B_1^2}{CA_1} + \frac{L_1^2}{C}\right) + 2(x_2^2 - y_2^2)\left(\frac{B_2^2}{CA_1} + \frac{L_2'^2}{C}\right)\right.$$
$$\left. + 4(x_1x_2 - y_1y_2)\left(\frac{B_1B_2}{CA_1} + \frac{L_1L_2'}{C}\right) - 2(x_1^2 + x_2^2)\right]. \tag{38}$$

Now we can plot the three-dimensional graphics of the Husimi function H_{OT} on the base of (38). From Fig. 8 and Fig. 9, we find that the plots of the Husimi function are different with the plots of the Wigner function because of the influence of the term ("coarse graining" function) $\exp[-\kappa|\sigma' - \sigma|^2 - \frac{|\gamma'-\gamma|^2}{\kappa}]$. In Fig. 8 we plot the Husimi function of the $OTCSS(H(\gamma_1,\sigma_1))$ for $\gamma_2 = 0$, $\sigma_2 = 0$, $\kappa = 1$ and $r = \pi/6, \pi/3$ respectively. Comparing with Fig. 8(a) and (b), parameter r doesn't influence the conformation of the figure except the value of $H(\gamma_1,\sigma_1)$, which is different from the Wigner function case. In Fig. 9 we plot the Husimi function of the $OTCSS(H(\gamma_1,\sigma_1))$ for $\gamma_2 = 0$, $\sigma_2 = 0$, $r = 0.1$ and $\kappa = 10, 1$ respectively. We find that with the squeezing parameter λ increasing, the peak value of the Husimi function of the *OTCSS* increase and the plot along σ_1 direction is squeezed, which is different from the Wigner function case.

In order to study the evolution law of the Husimi function more generally, we plot the two dimensional graphics of H_{OT} in Fig. 10. In Fig. 10(a) we study the law of Husimi function $H(\kappa)$ varying with parameter κ. We find that the value of $H(\kappa)$ increase with the value of κ and tend to steady in the end. In Fig. 10(b) we study the law of Husimi function $H(r)$ varying with parameter r. We find that the value of $H(r)$ decrease with parameter r and tend to zero in the end.

In summary, we calculate the Wigner function and Husimi function of the *OTCSS* and study their evolution law in this paper. We find that it is easy to calculate the Husimi function by virtue of the entangled two-mode Husimi operator $\Delta_h(\sigma,\gamma;\kappa) = |\sigma,\gamma\rangle_{\kappa\kappa}\langle\sigma,\gamma|$, which is presented in paper [17]. Owing to the existence of the term $\exp[-\kappa|\sigma' - \sigma|^2 - \frac{|\gamma'-\gamma|^2}{\kappa}]$

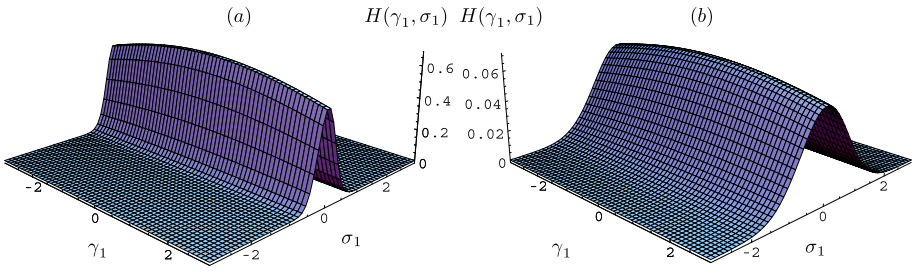

Fig. 9 The Husimi function of the OTCSS for $\gamma_2 = 0$, $\sigma_2 = 0$, $r = 0.1$ and different value of κ: (**a**) $\kappa = 10$, (**b**) $\kappa = 1$

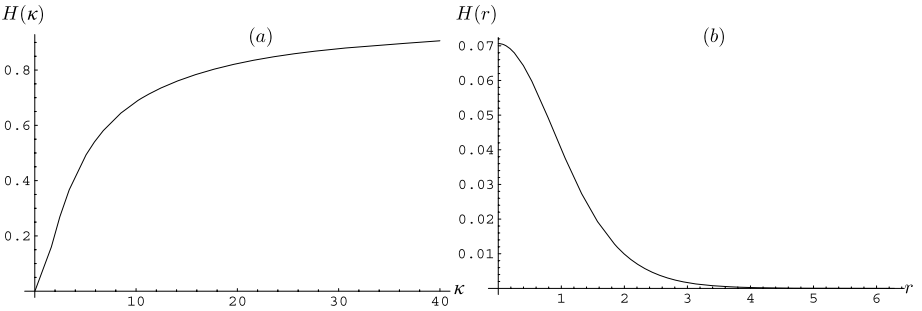

Fig. 10 **a** The Husimi function of the OTCSS varying with κ for $\gamma_1 = 0$, $\sigma_1 = 0$, $\gamma_2 = 0$, $\sigma_2 = 0$, $r = 0.1$. **b** The Husimi function of the OTCSS varying with r for $\gamma_1 = 0$, $\sigma_1 = 0$, $\gamma_2 = 0$, $\sigma_2 = 0$, $\kappa = 1$

in Husimi operator, the evolution law of the Husimi function is different from that of the Wigner function.

References

1. Loudon, R., Knight, P.L.: J. Mod. Opt. **34**, 709 (1987)
2. Bužek, V., Knight, P.L.: Prog. Opt. **34**, 1 (1995)
3. Bužek, V., Keitel, C.H., Knight, P.L.: Phys. Rev. A **51**, 2575 (1995)
4. Dodonov, V.V., Man'ko, V.I.: Theory of Nonclassical States of Light. Taylor & Francis, New York (2003)
5. Walls, D.F., Milburn, G.J.: Quantum Optics. Springer, Berlin (1994)
6. Bužek, V.: J. Mod. Opt. **37**, 303 (1990)
7. Fan, H.Y.: Phys. Rev. A **41**(3), 1526–1532 (1990)
8. Fan, H.-Y., Ruan, T.-N.: Sci. Sin. Ser. A **27**, 392 (1984)
9. Fan, H.-Y., Zaidi, H.R., Klauder, J.R.: Phys. Rev. D **35**, 1831 (1987)
10. Fan, H.-Y., Zaidi, H.R.: Phys. Rev. A **37**, 2985 (1988)
11. Fan, H.-Y.: Phys. Lett. A **126**, 145 (1987)
12. Fan, H.-Y.: Phys. Lett. A **126**, 150 (1987)
13. Fan, H.-Y.: Phys. Lett. A **127**, 403 (1987)
14. Wigner, E.: Phys. Rev. **40**, 749 (1932)
15. Husimi, K.: Proc. Phys. Math. Soc. Jpn. **22**, 264 (1940)
16. Fan, H.-Y., Yang, Y.-L.: Phys. Lett. A **353**, 439 (2006)
17. Fan, H.-Y., Guo, Q.: Phys. Lett. A **358**, 203–210 (2006)
18. D'Ariano, G.M., Rassetti, M.G., Katriel, J., Solomon, A.I.: In: Tombesi, P., Pike, E.R. (eds.) Squeezed and Nonclassical Light. Plenum, New York (1989)

19. Orszag, M.: Quantum Optics. Springer, Berlin (2000)
20. Schleich, W.P.: Quantum Optics in Phase Space. Wiley–Vch, Berlin (2001)
21. Scully, M.O., Zubairy, M.S.: Cambridge University Press, Cambridge (1997)
22. Dodonov, V.V.: J. Opt. B: Quantum Semiclass. Opt. **4**, R1–R33 (2002)
23. Fan, H.-Y.: Representation and Transformation Theory in Quantum Mechanics. Shanghai Scientific and Technical Publishers, Shanghai (1997) (in Chinese)